Electronic Supplementary Material (ESI) for Polymer Chemistry.

Supporting Information

Effect of Anions on the Phase Transition Temperature of Two structurally Isomeric Polymers: poly(*N*-isopropylacrylamide) and poly(2-isopropyl-2-oxazoline)

Taehun Chung, [a] *Jihoon Han,* [a] *Young Jae Kim,* [b] *Kyeong-Jun Jeong,* [b] *Jun Mo Koo,* [c] *Jemin Lee,* [d] *Hyung Gyu Park,* [d] *Taiha Joo,* [b] *and Youn Soo Kim* [*a,e]

a. *Department of Materials Science and Engineering, Pohang University of Science and Technology (POSTECH), 77 Cheongam-Ro, Nam-Gu, Pohang, Gyeongbuk 37673, Republic of Korea.*

   E-mail: ysookim@postech.ac.kr

b. *Department of Chemistry, Pohang University of Science and Technology (POSTECH), 77 Cheongam-Ro, Nam-Gu, Pohang, Gyeongbuk 37673, Republic of Korea.*

c. *Research Center for Bio-based Chemistry, Korea Research Institute of Chemical Technology (KRICT), Ulsan 44429, Republic of Korea.*

d. *Department of Mechanical Engineering, Pohang University of Science and Technology (POSTECH), 77 Cheongam-Ro, Nam-Gu, Pohang, Gyeongbuk, 37673, Republic of Korea.*

e. *Department of Chemical Engineering, Pohang University of Science and Technology (POSTECH), 77 Cheongam-Ro, Nam-Gu, Pohang, Gyeongbuk 37673, Republic of Korea.*

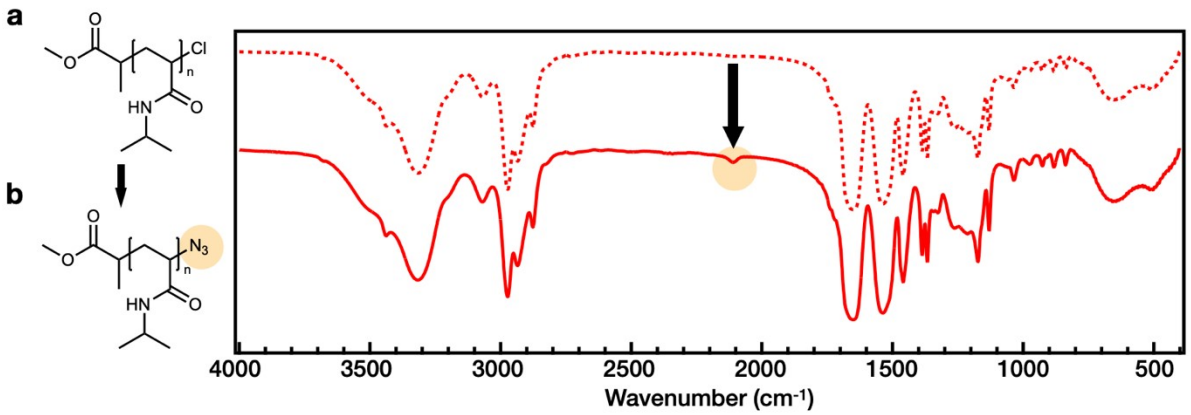

Fig. S1 FT-IR spectra obtained for (a) PNIPAAm-Cl, and (b) PNIPAAm-N_3.

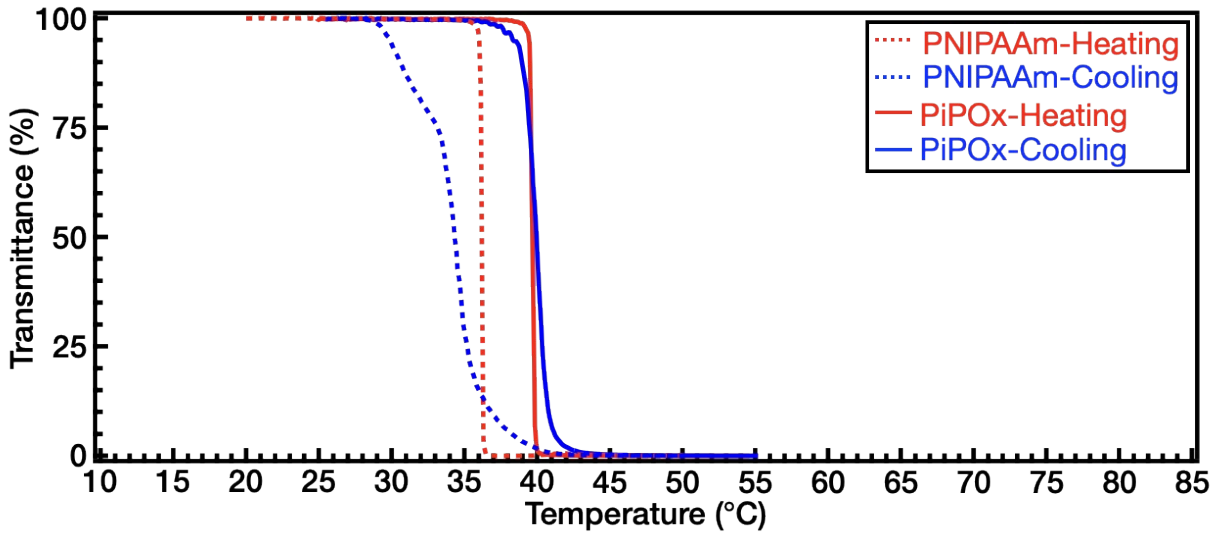

Fig. S2 Transmittance plots of PNIPAAm (dotted line) and PiPOx (solid line) as a function of temperature measured upon heating and cooling in DI water. Red lines; heating cycles, blue lines; cooling cycles. In all experiments, both the heating and cooling rates were set at 0.5 °C/min.

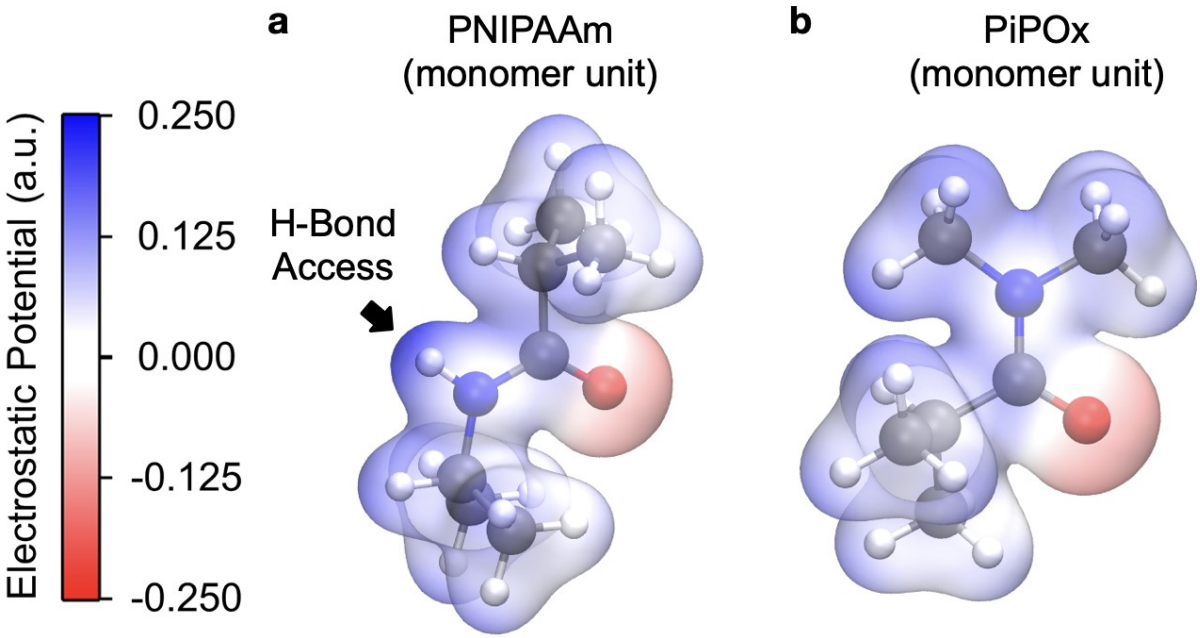

Fig. S3 Calculated electrostatic potential (ESP) distribution of the monomer units of (a) PNIPAAm, and (b) PiPOx in their optimized geometries. The proton of a hydrogen-bond donor in the PNIPAAm monomer is directed with arrow.

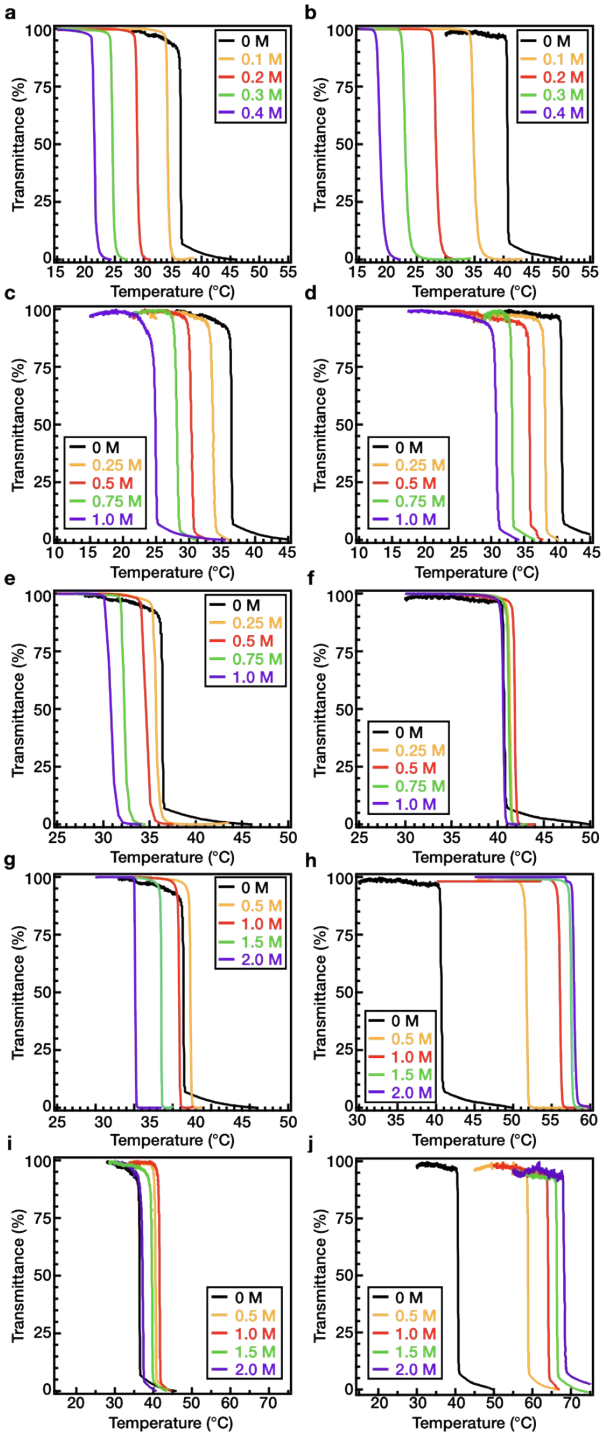

Fig. S4 Transmittance plots of (a) PNIPAAm and (b) PiPOx in Na_2SO_4 solution as a function of temperature. Transmittance plots of (c) PNIPAAm and (d) PiPOx in NaCl solution as a function of temperature. Transmittance plots of (e) PNIPAAm and (f) PiPOx in NaBr solution as a function of temperature. Transmittance plots of (g) PNIPAAm and (h) PiPOx in NaI solution as a function of temperature. Transmittance plots of (i) PNIPAAm and (j) PiPOx in NaSCN solution as a function of temperature. The concentration of the polymer was 1 wt%.

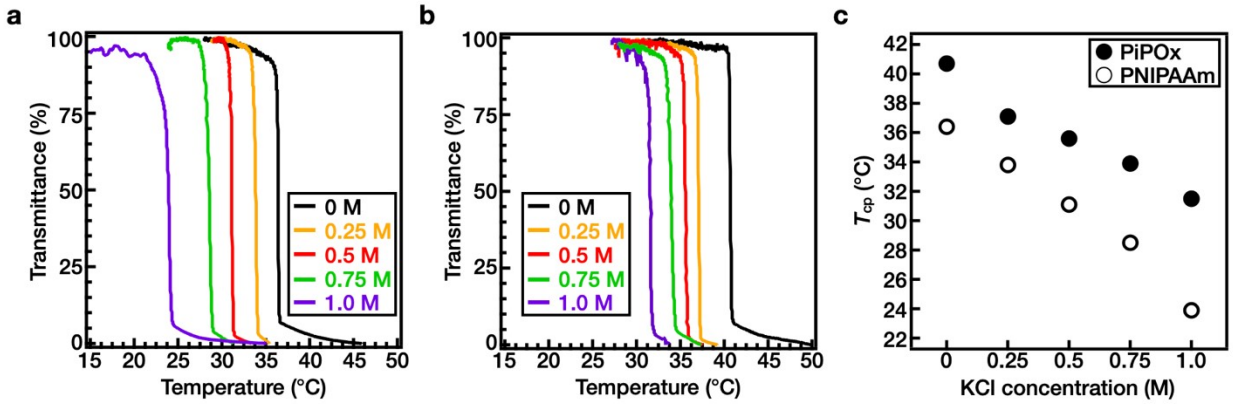

Fig. S5 Transmittance plots of (a) PNIPAAm and (b) PiPOx in KCl solution as a function of temperature. (c) T_{cp} profiles of PNIPAAm (open circle) and PiPOx (closed circle) in salt solutions as a function of KCl concentrations. The concentration of the polymer was 1 wt%.

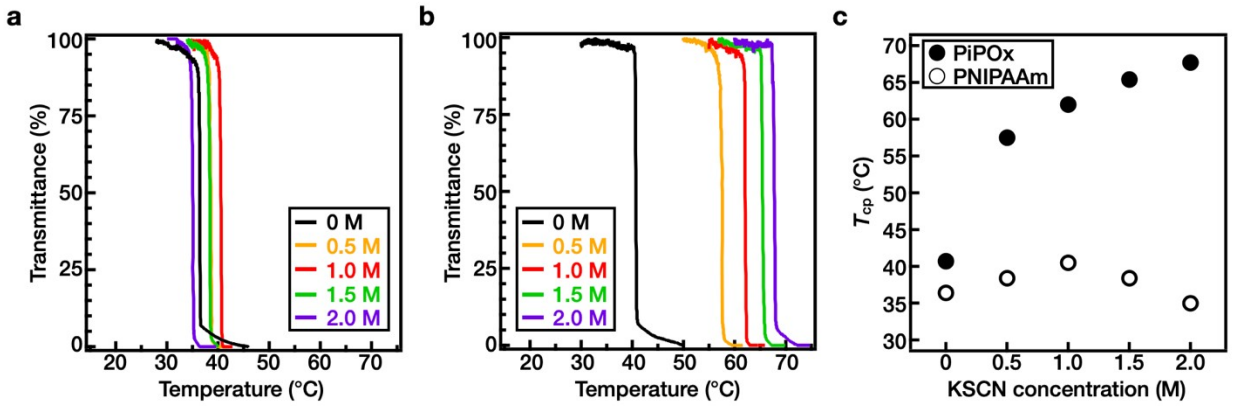

Fig. S6 Transmittance plots of (a) PNIPAAm and (b) PiPOx in KSCN solution as a function of temperature. (c) T_{cp} profiles of PNIPAAm (open circle) and PiPOx (closed circle) in salt solutions as a function of KSCN concentrations. The concentration of the polymer was 1 wt%.

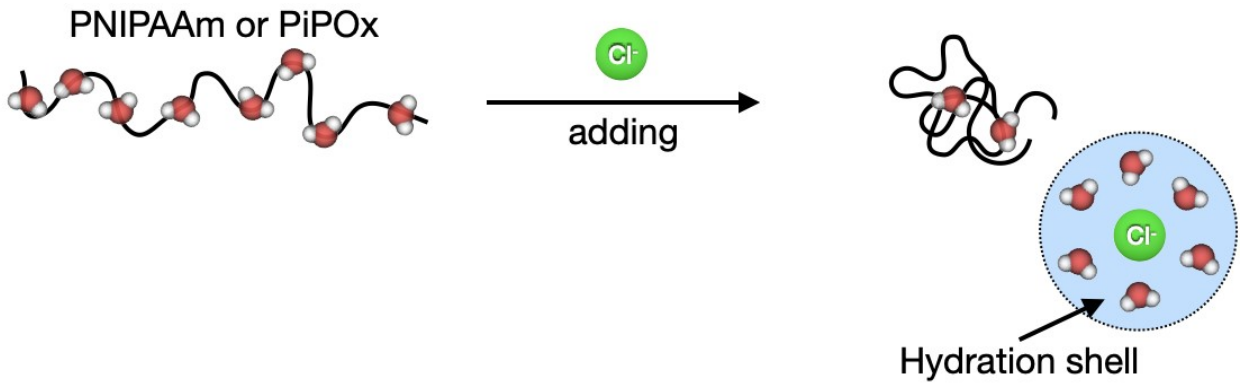

Fig. S7 Representative scheme of "salting-out" effect of PNIPAAm or PiPOx.

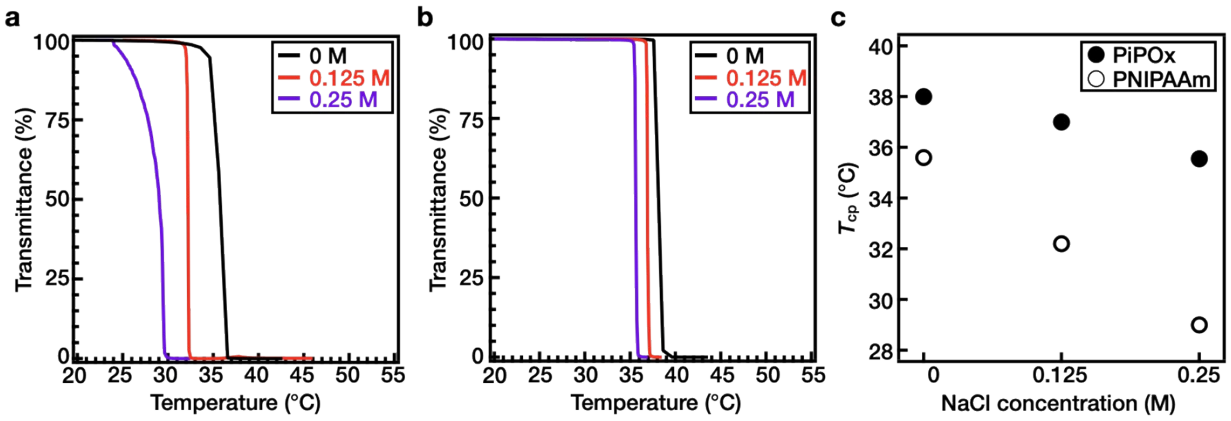

Fig. S8 Transmittance plots of (a) PNIPAAm and (b) PiPOx in NaCl solution as a function of temperature. (c) T_{cp} profiles of PNIPAAm (open circle) and PiPOx (closed circle) in salt solutions as a function of NaCl concentrations. The concentration of the polymer was 10 wt%.

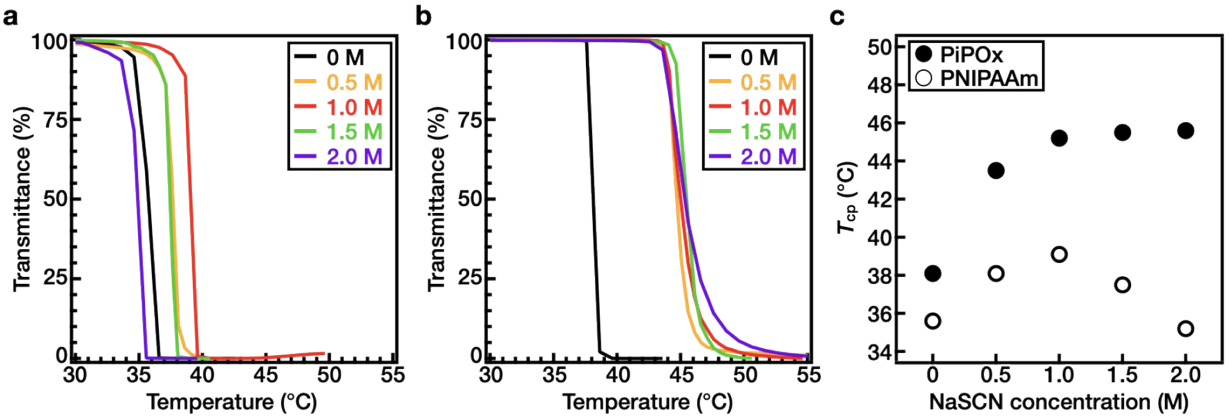

Fig. S9 Transmittance plots of (a) PNIPAAm and (b) PiPOx in NaSCN solution as a function of temperature. (c) T_{cp} profiles of PNIPAAm (open circle) and PiPOx (closed circle) in salt solutions as a function of NaSCN concentrations. The concentration of the polymer was 10 wt%.

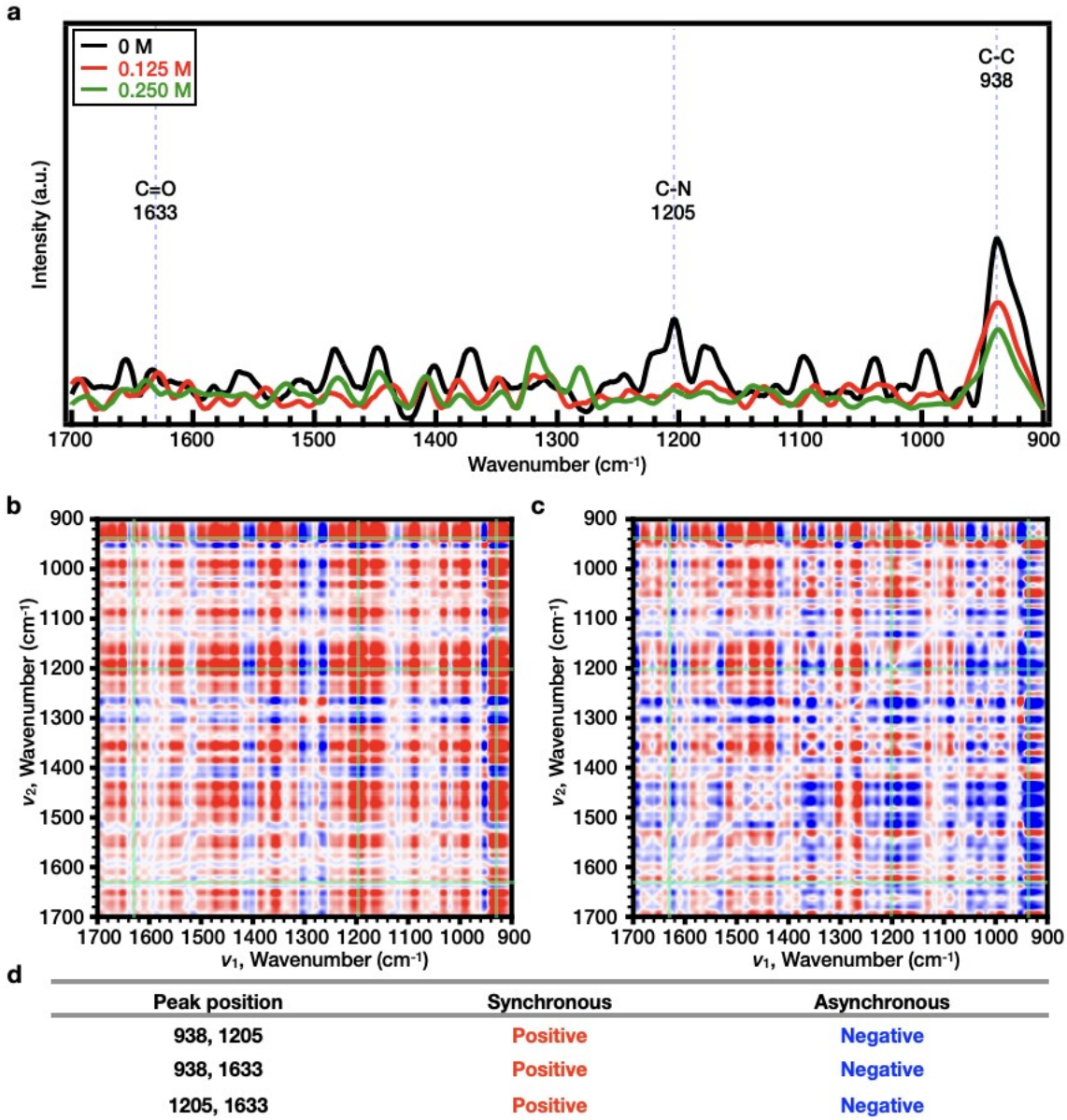

d

Peak position	Synchronous	Asynchronous
938, 1205	Positive	Negative
938, 1633	Positive	Negative
1205, 1633	Positive	Negative

Fig. S10 (a) RAMAN spectra of 10 wt% PNIPAAm solutions in D_2O (black line), 0.125 M NaCl (red line), and 0.250 M NaCl (green line). 2DCOS (b) synchronous and (c) asynchronous spectra of PNIPAAm (10 wt%) with variation in the NaCl concentration. (d) Peak descriptions for the 2DCOS results, where red is defined as a positive intensity, while blue is defined as a negative intensity.

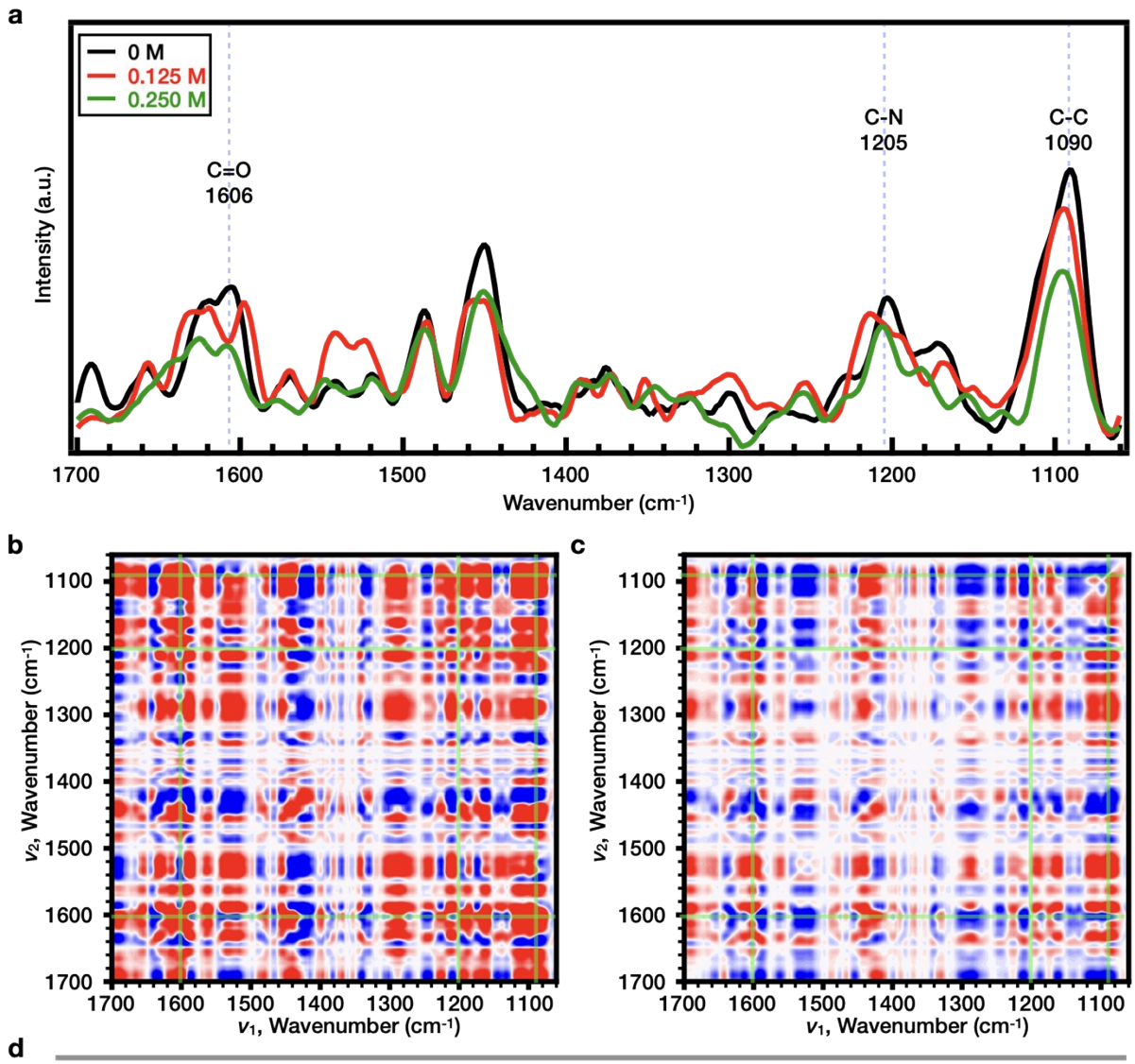

d

Peak position	Synchronous	Asynchronous
1090, 1205	Positive	Negative
1090, 1606	Positive	Negative
1205, 1606	Positive	Negative

Fig. S11 (a) RAMAN spectra of 10 wt% PiPOx solutions in D_2O (black line), 0.125 M NaCl (red line), and 0.250 M NaCl (green line). 2DCOS (b) synchronous and (c) asynchronous spectra of PiPOx (10 wt%) with variation in the NaCl concentration. (d) Peak descriptions for the 2DCOS results, where red is defined as a positive intensity, while blue is defined as a negative intensity.

Characterization method

Fourier-transform infrared spectroscopy (FT-IR)

FT-IR spectra were recorded in the range of 400–4000 cm^{-1} on FT-IR spectrometer (Nicolet iS50, Thermo Fisher Scientific) with a spectral resolution of 4 cm^{-1} and a total scan number of 32. All samples were freeze-dried, grinded, mixed with KBr, and pressed into pellets. To ensure an inert environment, all FT-IR cells were kept in an argon atmosphere (glove box), which excluded the effects of atmospheric water and CO_2 on FT-IR spectra.

Computational method

DFT calculations of electrostatic potential (ESP) distribution

Electrostatic potential (ESP) distributions were investigated by density functional theory (DFT) calculations performed on Gaussian 09 package[1] with B3LYP functional[2,3] and 6-31++G (d,p) basis set. The effect of water solvent was considered implicitly by the integral equational formalism polarizable continuum model (IEFPCM)[4]. Because of the limitation of system size available for DFT calculations, PNIPAAm and PiPOx were represented by their monomer units terminated with methyl groups at the truncated boundaries of the polymer backbone. In Figure S3, the ESP isosurfaces were depicted at electron density of 0.02 a.u.

References

1. M. J. Frisch, G. W. Trucks, H. B. Schlegel, G. E. Scuseria, M. A. Robb, J. R. Cheeseman, G. Scalmani, V. Barone, G. A. Petersson, et al., *Gaussian 09*, Revision A.02; Gaussian, Inc.: Wallingford, CT, 2010.

2. A. D. Becke, *J. Chem. Phys*., 1993, **98**, 5648−5652.

3. C. Lee, W. Yang, and R. G. Parr, *Phys. Rev. B*, 1988, **37**, 785−789.

4. E. Cancès, B. Mennucci, and J. Tomasi, *J. Chem. Phys*., 1997, **107**, 3032-3041.